



# High Frequency Model of PV Systems for the Evaluation of Ground Currents

M. C. Di Piazza<sup>1</sup>, F. Viola<sup>2</sup>, G. Vitale<sup>1</sup>

<sup>1</sup> Consiglio Nazionale delle Ricerche, CNR – ISSIA UOS Palermo

Via Dante, 12 90141 Palermo Phone +39 0916113513 Fax +39 0916113028, [dipiazza@pa.issia.cnr.it](mailto:dipiazza@pa.issia.cnr.it); [vitale@pa.issia.cnr.it](mailto:vitale@pa.issia.cnr.it)

<sup>2</sup>Università degli Studi di Palermo - DIEETCAM

viale delle Scienze, 90128 Palermo, Italy, (e-mail: [fabio.viola@unipa.it](mailto:fabio.viola@unipa.it)).

**Abstract.** A high frequency model of a photovoltaic (PV) plant is developed and analysed to investigate the common mode (CM) currents circulating through the ground connections of the plant. The modelling method is based on the measurement of the impedance frequency response of photovoltaic module and on a high frequency representation of the power conversion unit. An overall lumped parameters circuit model is obtained and then implemented in PSpice. The CM leakage currents are evaluated by simulation.

## Key words

High frequency modelling, Parameters identification, Photovoltaic plants, Common mode currents.

## 1. Introduction

In a photovoltaic plant, the power conversion unit (PCU) plays a key role, it achieves the tracking of the maximum power coming from the source and converts the available energy in a suitable form to be injected into the grid or to be utilized by the customer.

Several efforts have been made to set up Maximum Point Tracking (MPPT) algorithms [1], new power electronic devices and topologies [2-6].

On the other hand, the high speed commutation of power devices used in inverters for power conversion is responsible for very rapid voltages and currents transitions that lead to several serious problems such as conducted and radiated electromagnetic interference (EMI). Among the other possible adverse phenomena, there are overvoltages occurring at the inverter terminals when long cable configurations are used. One of the most critical disturbance is the common mode (CM) current, known also as “leakage current” or “ground current”. In a PV plant it can flow in a path formed by the source, the connection DC cables, the power converter and the grid by capacitive parasitic coupling with the ground connection. This current is responsible for electromagnetic interference (EMI) with other devices via the ground connection or for radiation phenomena. As a matter of fact, in a PV plant, there is usually a certain distance between the PV source and the power converter and, in some cases, the common mode current

path can be compatible with a multiple of the wavelengths its spectrum is composed of.

Few papers dealing with this problems are present in literature, however they describe accurately the common mode current generation. In particular in [7] phenomena and coupling mechanisms dealing with a high power grid connected plant are pointed out by means of an equivalent circuit and through measurements. [8] and [9] deal with single-phase transformerless systems in which the absence of a low frequency transformer allows a galvanic connection between the grid and the plant and the common mode current towards the grid is limited only by the EMI inverter filter. Both these papers propose a common mode equivalent model for the single-phase grid connected inverter at medium frequency range and analyse several topologies.

This paper focuses the attention on the role of parasitic components, they are mainly stray capacitances in the PV source and in the inverter, parasitic inductances in the wires connecting the inverter power devices and parasitic components inside power devices.

An accurate high frequency modelling of the plant allows the CM current to be predicted.

The paper is organized as follows: in section 2 the high frequency parasitic parameters present in a PV plant are described, section 3 is dedicated to the experimental set up used to identify the PV module parasitic parameters, section 4 contains the details of PSpice implementation of the model for simulation, finally results are given and discussed in section 5.

## 2. Photovoltaic Plant Layout

A PV plant mainly consists of a PV source composed of a series/parallel connection of PV modules and a PCU in which usually a DC/DC converter provides the MPPT and the matching of voltage between the source output and the inverter input. An inverter stage is then connected to the grid via a series inductance, a low frequency (LF) transformer and an EMI filter. The block diagram is drawn in Figure 1.

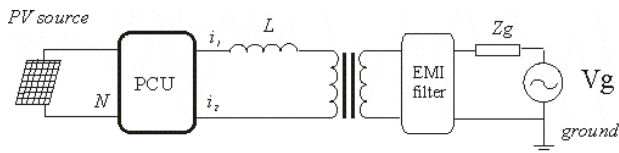


Fig. 1. General block diagram of a PV plant.

The current to be injected into the grid is given by the coupling inductance as the difference between the inverter voltage, seen as a voltage controlled source, and the grid voltage, divided by its impedance.

The transformer assures galvanic isolation between the grid and the PV plant, providing personal protection. It can be used to raise the voltage given by the inverter and to avoid direct current to be injected into the grid, which could saturate the distribution transformer. On the other hand, the LF transformer increases the weight and cost of the PV plant, for this reason, especially for low power applications and according to the Standards of some countries, it can be eliminated. This last solution is known as transformerless plant.

With reference to Figure 1, the CM voltage at the inverter output is defined assuming as common reference the negative point of DC bus  $N$ , as:

$$v_{cm} = \frac{v_{1N} + v_{2N}}{2} \quad (1)$$

The differential mode (DM) voltage is the output inverter voltage:

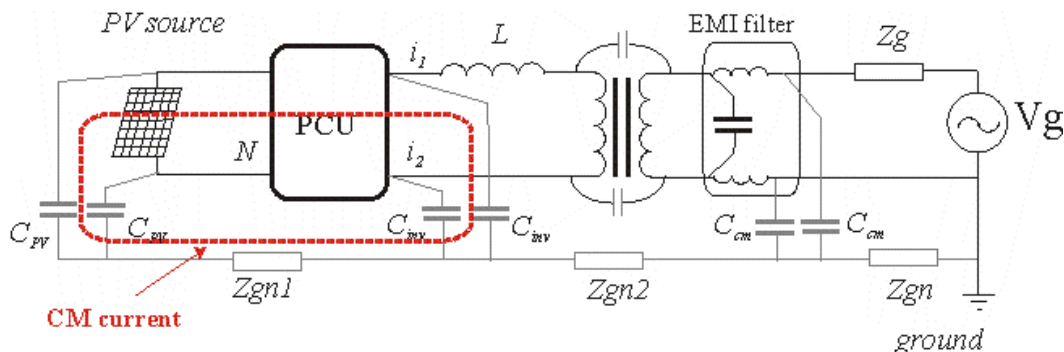


Fig. 2. High frequency representation of a PV plant.

It can be noted that the high frequency modelling points out all possible paths for CM current. However the LF transformer, when present, exhibits a high impedance at CM current frequencies, therefore, the main path to be investigated is formed by stray capacitances between the PV source and the inverter.

### 3. PV Module Parasitic Parameters Identification

The value of parasitic capacitance between the PV source and the ground is affected by the installation characteristics; therefore, a parameter identification on the real PV source is necessary to correctly define the high frequency model.

The experimental identification has been performed here on a single module. The considered module is a

$$v_{dm} = v_{1N} - v_{2N} = v_{12} \quad (2)$$

The CM current is the sum of the two line output current:

$$i_{cm} = i_1 + i_2 \quad (3)$$

And the DM current is given by:

$$i_{dm} = \frac{i_1 - i_2}{2} \quad (4)$$

From Figure 1 it can be noticed that the DM current corresponds to the current injected into the grid by the inverter and the CM current is a current that finds a path through the parasitic capacitive couplings between the different parts of the PV plant and the ground connection. For this reason, it is known also as ground current.

In the PV plant representation given in Figure 1, no path for CM current exists. The possible paths are noticeable by using a high frequency modelling for the plant as that schematized in Figure 2. These paths include stray capacitances between the PV source and the ground  $C_{pv}$ , stray capacitances between the line output inverter and the ground  $C_{inv}$  and stray capacitances of the EMI filter,  $C_{cm}$ . The ground path impedance is indicated with  $Z_{gn}$ .

monocrystalline type; its characteristic parameters are shown in Table I.

Table I: Characteristics of the PV module

Nominal power	$P_n$	20 W
Short circuit current	$I_{sc}$	9.34 A
Open circuit voltage	$V_{oc}$	21 V
Maximum power point current	$I_{MPP}$	1.18 A
Maximum power point voltage	$V_{MPP}$	16.8 V

It should be observed that, the modelling of a PV array can be achieved considering the actual PV modules connection or performing measurements directly on the whole installation to consider the coupling with the metallic support and the ground, for example.

The experimental set up comprises an Agilent 4285A LCR meter; it is connected between the two input terminals of the PV source and the ground.

A dedicated software, implemented by LabView on a PC, controls the RCL meter to acquire the measured impedance values from 75 kHz to 4 MHz.

The measurement arrangement scheme is shown in Figure 3. The curve of the acquired impedance is given in Figure 4. It should be noted that up to 500 kHz the curve shows a purely capacitive behaviour, then an inductive contribution is present. By a fitting procedure on measured data in the range 100 kHz- 4 MHz, the parasitic capacitance value is calculated to be equal to 73 pF.

Performing a further measurement from 1 MHz to 7 MHz, only a parasitic inductance is individuated, whose value is about 1  $\mu$ H. A small parasitic resistance due to the connection is present but it is neglected in this analysis.

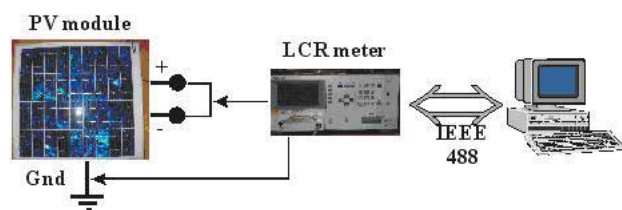


Fig. 3. Measurement arrangement for the evaluation of a PV module parasitic components.

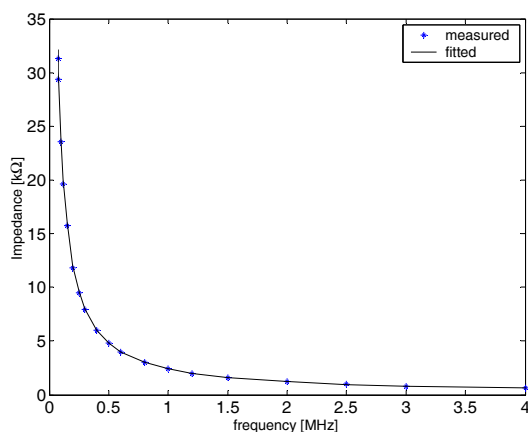


Fig. 4. Measured Impedance curve.

## 4. HF model Implementation

Each component of the PV plant, shown in Figure 2, has been modelled according to the need for a high frequency analysis. The obtained complete model is then implemented in PSpice software.

### A. PV array

As for the PV array, it is imposed that it should supply a voltage of about 500V to the inverter and a power of about 1 kW to the grid. In order to satisfy these requirements with modules having the characteristics given in Table I, two parallel connected strings, each formed of 24 series connected modules are needed. On the basis of this configuration of the complete array, the parasitic parameters previously determined for one module are re-calculated. From the point of view of the common mode behaviour, all parasitic capacitors and inductors are parallel connected, as a consequence, the

parasitic capacitance of one module is multiplied and the parasitic inductance is divided for the number of utilized modules, respectively. The values reported in Table II are obtained. Since the proposed analysis is focused on the evaluation of the ground currents propagation, a simplified representation of the PV generator is chosen. In particular, each PV module is schematised as an ideal voltage source supplying the voltage  $V_{oc}$  with a series resistance to account for the voltage drop in the semiconductor. Considering that the module should supply at any instant the voltage of the MPP under Standard Test Conditions, i.e., 16.8 V, the series resistance can be determined according to (5).

$$R_{pv} = \frac{V_{oc} - V_{mpp}}{I_{mpp}} \approx 4\Omega \quad (5)$$

For the complete PV array the value of this series resistance will be 48  $\Omega$ . The PSpice model of the PV array is a very simple circuit; it is shown in Figure 5.

Table II: Parasitic parameters of the PV array

Parasitic capacitance to ground	$C_{pv}$	1.75 nF
Paratic inductance of the connecting cables	$L_{pv}$	41.6 nH

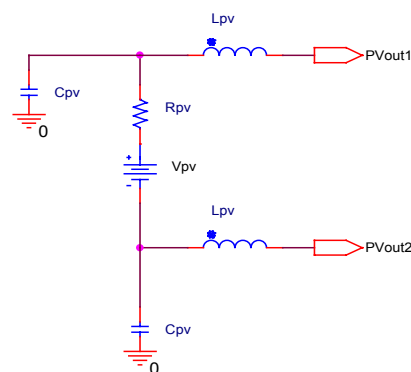


Fig. 5. PSpice model of the PV array.

### B. Power Conversion Unit

The power conversion unit is a full-bridge single phase IGBT inverter, operating in SPWM mode with a switching frequency of 10 kHz and a modulation index of 0.8. In order to study the CM current propagation in the loop between the PV array and the inverter, a high frequency circuit model of the inverter is developed, including all the parasitic parameters. In particular the stray capacitance between the IGBT modules, the ground connected heatsink and the stray inductance of the connecting wires of each leg of the inverter have been considered. The values of the parasitic capacitances are measured by a precision RLC meter (Agilent 4285ALCR) in a frequency range between 150 kHz and 4 MHz. The value of the stray inductance of the connecting wires  $L_{inv}$  is dependent on the converter layout and is evaluated using the analytical formula for two parallel cylindrical conductors. The PSpice model of the inverter is shown in Figure 6. The parasitic parameters values are reported in Table III.

Table III: Parasitic parameters of the inverter

Parasitic capacitance to ground	$C_{inv}$	150 pF
Paratic inductance of the connecting wires	$L_{inv}$	10 nH

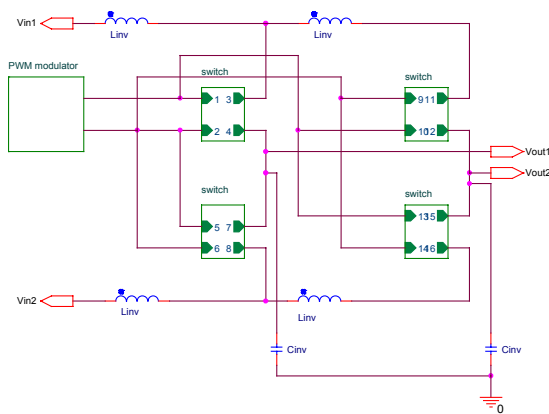


Fig. 6. PSPice model of the inverter.

### B. Power Devices

As for each IGBT, it is represented in a simplified way as an ideal switch, in series with an L-R branch formed of a conduction parasitic inductance,  $L_{on}$ , and a resistance  $R_s$  that considers the commutation losses. In addition an R-C branch is connected in parallel to properly model the commutation speed of the power device. In Figure 7 the model of the single IGBT is shown. The values of the parasitic parameters of the IGBT are given in Table IV.

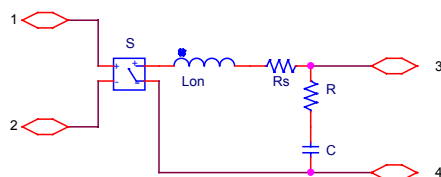


Fig. 7. PSPice model of the IGBT

Table IV: Parasitic parameters of the inverter

Conduction parasitic inductance	$L_{on}$	10 nH
Series resistance	$R_s$	0.1 $\Omega$
Shunt Resistance	R	100 k $\Omega$
Shunt capacitance	C	1 nF

It has been demonstrated in the case of a power drive that, for cable lengths up to 10 m, the parasitic parameters of the connecting cables do not influence significantly the CM propagation within the system at

frequencies up to 10 MHz [10]. Therefore, if the inverter is supposed to be close to the PV panel, the models of cables can be neglected without affecting the validity of the analysis.

In this paper the effect of the connecting cables are not considered.

## 5. Results

On the basis of the modelling described in the previous sections, a global circuit model of the PV plant has been defined and implemented in PSPice. It is useful for the prediction of CM currents. In this model the PV plant is supposed to be grid connected through a line inductance  $L=6\text{mH}$ . The corresponding circuit scheme is depicted in Figure 7. The grid is simply represented by a sinusoidal generator  $V_g$ , a resistive load  $R_l$  and on ohmic-inductive branch  $R_g-L_g$  accounting for the connection cables. Figure 8 shows the PSPice model of the overall grid connected plant. No parasitic couplings through ground are considered on the grid side; this case is very likely when a LF transformer is present in the plant.

The basic waveforms of the PV plant operation are obtained by simulations. In Figure 9 the voltage at the output of the inverter is shown. Figure 10 shows a zoom of this voltage, where one of the rapid transitions due to commutation is put in evidence. Figure 11 illustrates the current on inductance  $L$ , whose value guarantees that the PV plant is supplying power to the grid.

The CM voltage in a period 20 ms is given in Figure 12; Figure 13 shows a particular of such a CM voltage, i.e., the single pulse corresponding to a device commutation. It should be noted that, even in time domain representation, the presence of oscillations due to PWM explains the presence of high frequency voltage harmonics. These harmonics supply a loop formed by capacitors and inductors that is a resonant circuit in which the common mode current will flow. The frequency spectrum of the CM voltage is shown in Figure 14. It presents harmonics at frequencies multiple of the switching frequency and strong resonance at about 12 MHz. Figure 15 shows the CM current in the loop between the PV array and the inverter in a period 20 ms, while Figure 16 is the zoom of a single CM current pulse.

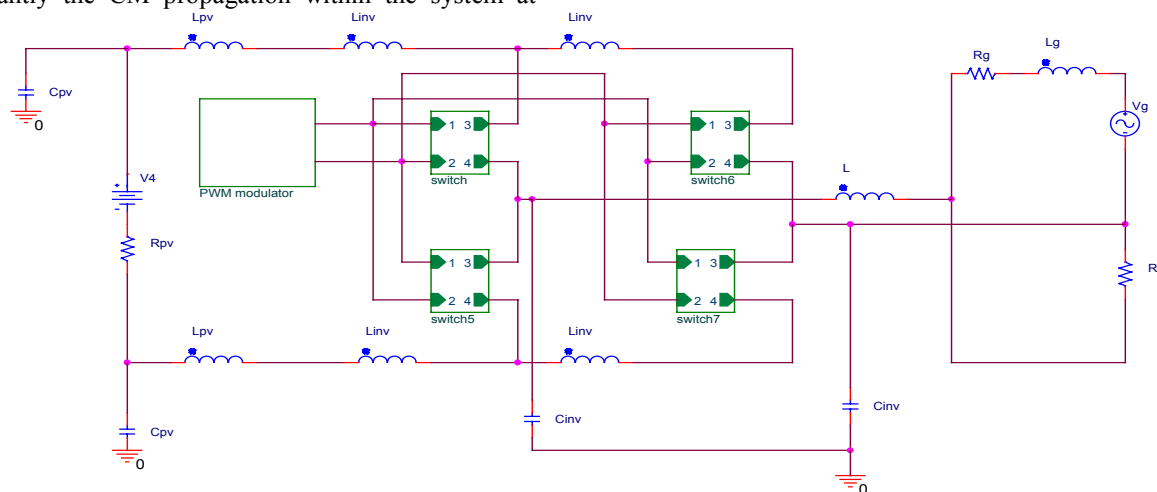


Fig. 8. PSPice global model of the grid-connected PV plant.

Both Figures confirm the presence of oscillation in CM current. In particular, in the waveform of Figure 15, it can be noted that its envelope has a period corresponding to twice the grid frequency. In Figure 16 the zoom of a single pulse highlights the absence of DC components as expected and the typical behaviour of a damped resonant circuit; the frequency of the oscillation is equal about to 80 ns.

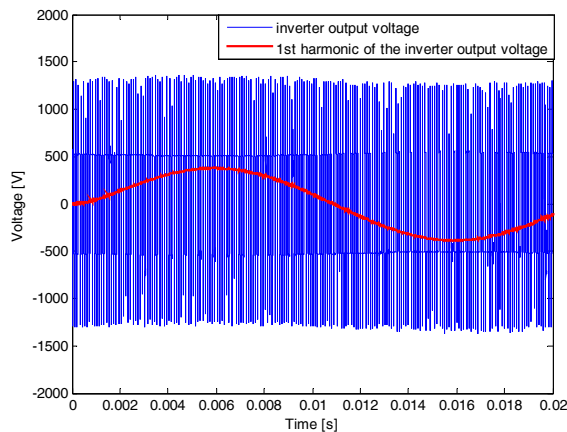


Fig. 9. Voltage at the output of the inverter.

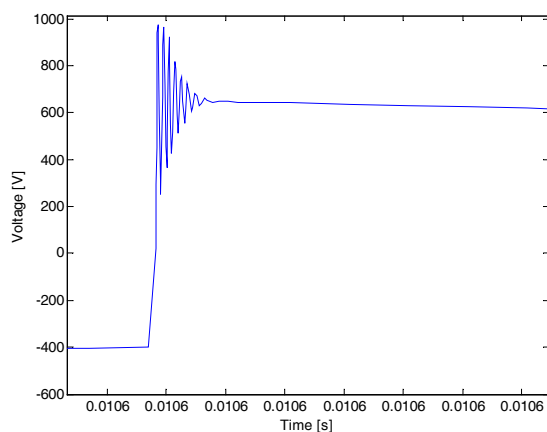


Fig. 10. Zoom of the voltage at the inverter output.

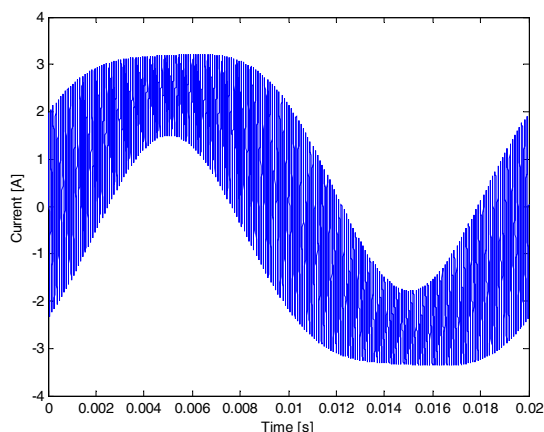


Fig. 11. Current on the line inductance.

It has the same order of magnitude of the period obtained by  $T = 2\pi\sqrt{L_{pv}C_{pv}} = 53$  ns. On this basis, one can state that the parasitics of the PV array are the parameters that mainly affect the CM current propagation. Finally, Figure 17 shows the frequency spectrum of the CM current, where the resonance at 12 MHz is present, as well.

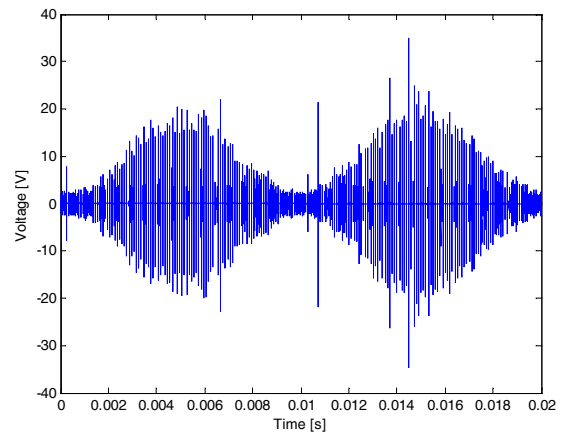


Fig. 12. CM voltage at the inverter output.

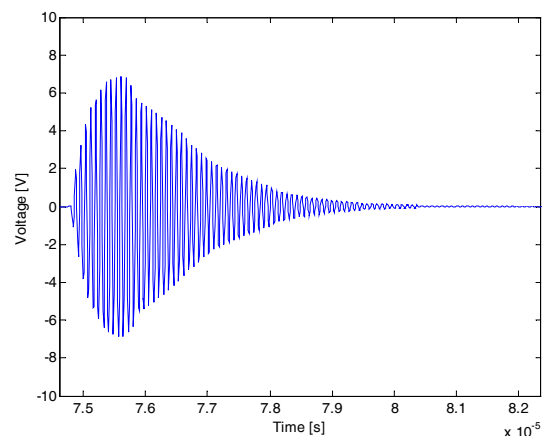


Fig. 13. Single pulse in the CM voltage.

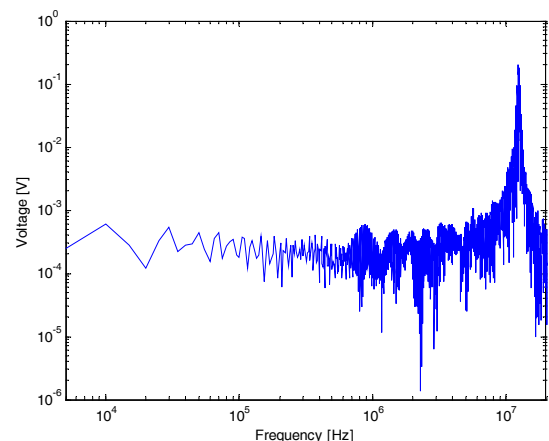


Fig. 14. Frequency spectrum of the CM voltage.



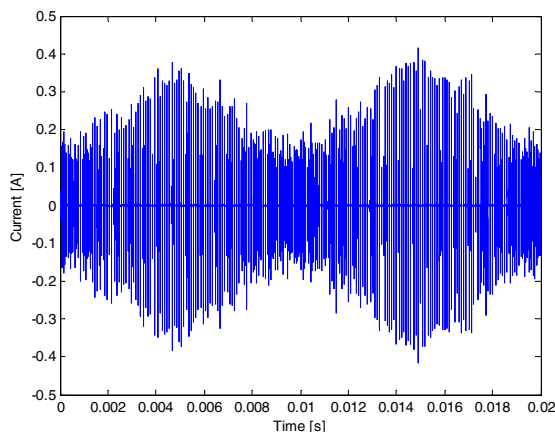


Fig. 15. CM current in the loop between the PV array and the inverter.

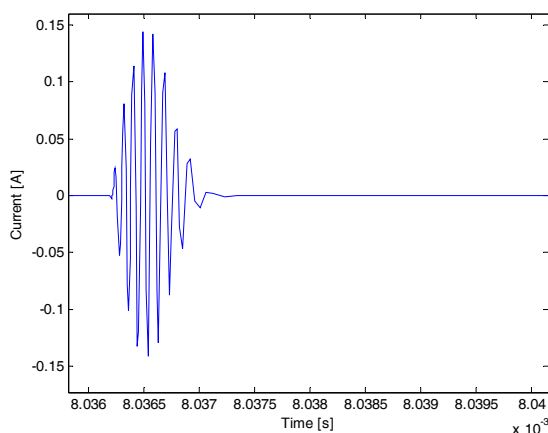


Fig. 16. Single pulse in the CM current.

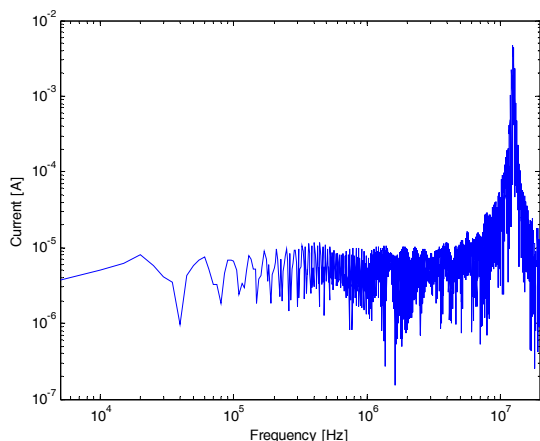


Fig. 17. Frequency spectrum of the CM current.

## 6. Conclusion

In this paper a high frequency circuit model of a PV plant has been developed to be used for CM current propagation analysis. The main parts of the plant have been modelled using a lumped parameter approach; in particular, the PV array has been modelled on the basis of experimental results obtained on a single module in a laboratory test bench. The whole PV plant model has been implemented in PSpice software and the CM currents have been obtained in simulation both in time and frequency domain.

The analysis of the results puts in evidence that the parasitic parameters of the PV generator form a resonant circuit whose frequency is present in the CM current excited by the CM voltage. It has been observed that the resonance is mainly tied to the PV source stray capacitance and cable inductance; therefore the plant layout is the main aspect to be considered when predicting the CM currents.

## Acknowledgement

The Authors want to acknowledge Ms Stefania Collura who did preliminary analysis on CM current propagation in PV plants as a part of her BSc thesis.

## References

- [1] T. Esram, P. L. Chapman, "Comparison of Photovoltaic Array Maximum Power Point Tracking Techniques", IEEE trans on Energy C., vol. 22, n. 2, June 2007
- [2] F. Iov, F. Blaabjerg, "Power Electronics for Renewable Energy Systems", POWERENG 2009 Lisbon, Portugal, March 18-20, 2009
- [3] Frede Blaabjerg, Florin Iov, Remus Teodorescu, Zhe Chen, "Power Electronics in Renewable Energy Systems", EPE-PEMC 2006, Portoroz, Slovenia.
- [4] S. B. Kjaer, J. K. Pedersen, F. Blaabjerg, "A Review of Single-Phase Grid-Connected Inverters for Photovoltaic Modules", IEEE trans on Industry Applications, vol. 41, n. 5, September/October 2005.
- [5] J. M. Carrasco, L. Garcia Franquelo, J. T. Bialasiewicz, E. Galván, R. C. Portillo Guisado, M. Á. Martín Prats, J. I. León, N. Moreno-Alfonso, "Power-Electronic Systems for the Grid Integration of Renewable Energy Sources: A Survey", IEEE trans. On Industrial Electronics, vol. 53, n. 4, August 2006.
- [6] R. Gonzalez, J. Lopez, P. Sanchis, and L. Marroyo, "Transformerless inverter for single-phase photovoltaic systems," IEEE Trans. Power Electron., vol. 22, no. 2, pp. 693–697, Mar. 2007.
- [7] R. Araneo, S. Lammens, M. Grossi, S. Bertone, "EMC Issues in High-Power Grid-Connected Photovoltaic Plants", IEEE trans on Electromagnetic compatibility, vol. 51, n. 3, August 2009.
- [8] H. Xiao, S. Xie, "Leakage Current Analytical Model and Application in Single-Phase Transformerless Photovoltaic Grid-Connected Inverter", IEEE trans on Electromagnetic compatibility, vol. 52, n. 4, Nov. 2010
- [9] E. Gubia, P. Sanchis, A. Ursua, J. Lopez, and L. Marroyo, "Ground current in single-phase transformerless photovoltaic systems," in Progress in Photovoltaics: Research and Applications. New York: Wiley, pp. 629–650, 2007.
- [10] M. C. Di Piazza, A. Ragusa, G. Vitale, "Design of Grid-Side Electromagnetic Interference Filters in AC Motor Drives with Motor-Side Common Mode Active Compensation", IEEE Transactions on Electromagnetic Compatibility, vol. 51, N. 3 Part 2, August 2009, Page(s):673 – 682.